PREPRINT UCRL-82867

CONF-800613--4

Lawrence Livermore Laboratory

ON THE SPURIOUS PRESSURES GENERATED BY CERTAIN GFEM SOLUTIONS OF THE INCOMPRESSIBLE NAVIER-STOKES EQUATIONS

R. L. Sani, P. M. Gresho and R. L. Lee

October 15, 1979

Prepared for the Third International Conference on Finite Element in Flow Problems, Banff, Alberta, Canada, June 10-13, 1980.

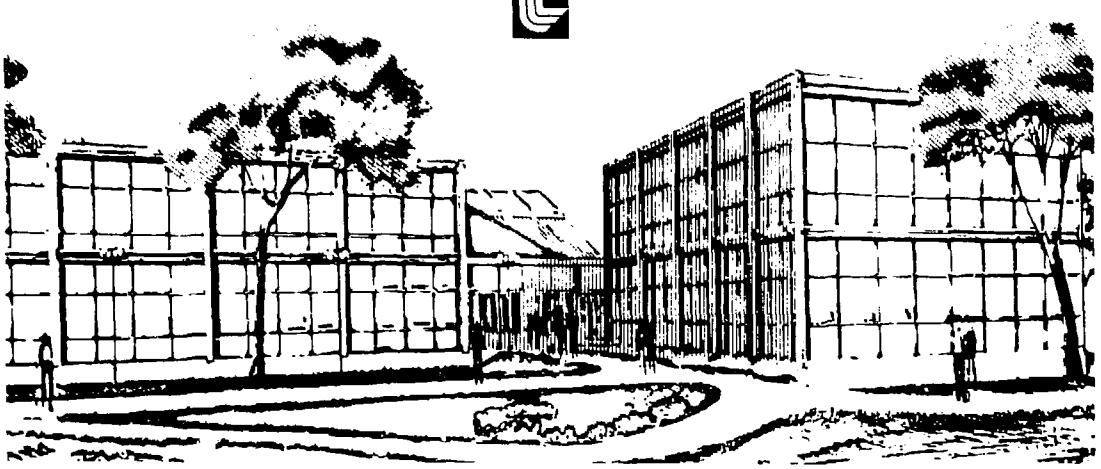

ON THE SPURIOUS PRESSURES GENERATED BY CERTAIN GFEM SOLUTIONS OF THE INCOMPRESSIBLE NAVIER-STOKES EQUATIONS

by

R. L. Sani
Department of Chemical Engineering
Cooperative Institute for Research
in Environmental Sciences
University of Colorado/NOAA
Boulder, Colorado 80309

P. M. Gresho and R. L. Lee
Lawrence Livermore Laboratory
University of California
Livermore, California 94550

ABSTRACT

The spurious pressures and acceptable velocities generated when using certain combinations of velocity and pressure approximations in a Galerkin finite element discretization of the primitive variable form of the incompressible Navier-Stokes equations are analyzed both theoretically and numerically for grids composed of quadrilateral finite elements. Schemes for obtaining usable pressure fields from the spurious numerical results are presented for certain cases.

INTRODUCTION

Discretized approximations to the incompressible Navier-Stokes equations, in the primitive variable (velocity-pressure) formulation, especially when generated via the Galerkin finite element method (GFEM) have been plagued with confusion regarding the "appropriate" workable combination of velocity and pressure approximations. Since the early observations of Hood and Taylor [1], in which spurious pressure solutions were generated when the same basis functions were used for pressure and velocity on conforming quadrilateral elements, but not when using mixed interpolation (pressure one order lower than velocity), most GFEM practitioners have accepted this necessity and adhered to it. The explanation in [1], cast in terms of the "balancing of residuals" from momentum and continuity equations, was judged inadequate by Olson and Tuann [2] who explained it in terms of the eigenvalues of a single element - herein both of these explanations are shown to be inadequate.

Even when mixed interpolation is employed, numerical difficulties can be encountered; for example, piecewise linear approximation for velocity and piecewise constant approximation for pressure has been found to work poorly in some cases [3-6]. The solutions sometimes display acceptable velocities but totally spurious pressures which are afflicted with the "checkerboard (CB) syndrome," wherein pressure oscillations occur which are frequently of one sign on all "black" elements and of the opposite sign on all "red" elements.

Herein we will focus on this problem for 2-D grids composed of quadrilateral finite elements and will define and characterize this behavior, both theoretically and numerically, in terms of "zero energy pressure modes," and present some simple methods for extracting good physical pressures from polluted numerical results in certain cases. Our techniques are useful in 3D calculations [7] as well as in some finite difference techniques [8], [9]. Detailed analyses and results, summarized in this paper, will be available in the near future [10].

CONTINUUM EQUATIONS AND THEIR GFEM DISCRETIZATION

The setting for our discussion will be the steady Stokes equations:

$$\nabla \cdot \underline{\underline{\tau}} = \underline{0} \ , \qquad \nabla \cdot \underline{u} = 0 \ , \tag{1a, 1b}$$

where $\tau_{ij} = -p\,\delta_{ij} + S_{ij}$ is the symmetric stress tensor, $S_{ij} = \mu\left(\frac{\partial u_i}{\partial x_j} + \frac{\partial u_j}{\partial x_i}\right)$ $\underline{u} = (u, v)$ is the velocity, p is the pressure and μ is the (constant) viscosity of the fluid. The results presented herein also apply to unsteady, nonlinear (viscous or inviscid), and nonisothermal (Boussinesq) flows.

The GFEM discretized approximation is applied to the weak form of (1): viz,

$$\int_\Omega \underline{\underline{\tau}} \cdot \nabla\phi_i = \int_{\partial\Omega} \phi_i \underline{\underline{\tau}} \cdot \underline{n} \quad , \quad i = 1, 2, \ldots, N; \qquad \int_\Omega \psi_i \nabla \cdot \underline{u} = 0 \quad , \quad i = 1, 2, \ldots, M; \tag{2a,2b}$$

over the domain Ω with boundary $\partial\Omega$ where $\underline{n}$ is the outward pointing unit normal vector, $\underline{\underline{\tau}} \cdot \underline{n}$ is the surface traction, ϕ_i represents any basis function for velocity, and ψ_i is any basis function for pressure. Inserting the following appropriate piecewise polynomial basis function expansions,

$$u_i^h = \sum_{k=1}^{N_i} u_i^k \phi_k(\underline{x}) \quad , \quad i = 1, 2; \qquad p^h = \sum_{k=1}^{M} p_k \psi_k(\underline{x}), \tag{3a, 3b}$$

into (2) leads to the GFEM equations [11] ,

$$\underline{\underline{K}}\,\underline{U} + \underline{\underline{C}}\,\underline{P} = \underline{f} \quad , \qquad \underline{\underline{C}}^T \underline{U} = \underline{g} \quad , \tag{4a, 4b}$$

where $\underline{U} = (u_1, u_2, \ldots, u_{N_1}, v_1, v_2, \ldots, v_{N_2})^T$, $N = N_1 + N_2$, $\underline{P} = (p_1, p_2, \ldots, p_M)^T$, $\underline{\underline{K}}$ is a positive-definite symmetric matrix, and $\underline{\underline{C}}$ is an unsymmetric and indefinite rectangular matrix, which is the "cause" of the problem addressed herein. The vectors $\underline{f}$ and $\underline{g}$ reflect the effect of the imposed boundary conditions; $\underline{f}$ could represent not only prescribed boundary forces but also velocities, whereas $\underline{g}$ corresponds only to prescribed velocities. (The specification of pressure boundary conditions is inappropriate and is not considered herein; see [11]).

C^0 BILINEAR VELOCITY-PIECEWISE CONSTANT PRESSURE ELEMENT

In order to motivate our discussion of more complicated elements, we will first consider this "simple" special case. Here the discretized continuity equation (4b) guarantees a mass balance on each element in the mesh. These mass balances, in conjunction with the imposed boundary conditions, can lead to what are termed "pressure modes" which correspond to special solutions of (4) with $\underline{f} = \underline{0}$ and $\underline{g} = \underline{0}$ for which $\underline{U} = \underline{0}$ and $\underline{\underline{C}}\,\underline{P} = \underline{0}$ for nontrivial $\underline{P}$. These solutions may be spurious in that they do not correspond to physical pressures which, in numerical simulations, are often buried in the "noise level" since these modes cause the overall coefficient matrix to be singular. For this particular element, there are two pressure modes which can exist; one of these can exist on any (isoparametric) mesh, and the other, on a mesh composed of parallelograms.

A. Hydrostatic Pressure Mode

This physical mode is more general than the (spurious) CB mode, in that it can occur for any type of velocity and pressure approximation and for any domain subdivision. Its existence depends solely on boundary conditions.

The discretized continuity equations (2b) may be summed to arrive at the global mass balance

$$\int_\Omega \nabla \cdot \underline{u}^h = \int_{\partial\Omega} \underline{n} \cdot \underline{u}^h = 0 \quad . \tag{5}$$

This constraint among normal velocity components of the boundary modes must be satisfied by the numerical solutions. For example, for the simple grid represented in Fig. 1, the constraint equation takes the form

$$(u_4-u_1)h_1 + (u_8-u_5)(h_1+h_2) + (u_{12}-u_9)h_2 + (v_9-v_1)\ell_1 + (v_{10}-v_2)(\ell_1+\ell_2) + (v_{11}-v_3)(\ell_2+\ell_3)$$
$$+ (v_{12}-v_4)\ell_3 = 0 \quad . \tag{6}$$

Consideration of possible applied boundary conditions (BC's) then leads directly to the following conclusions (assuming at this point, that no other pressure modes exist):

1. If the imposed BC's do not imply a constraint among normal velocities on the entire boundary (i.e., normal tractions specified on a portion of $\partial\Omega$) then (5) is independent and required and there is no hydrostatic pressure mode. (The pressure datum is set by the normal traction boundary condition).

2. If the imposed BC's satisfy (i.e., duplicate) Eqn. (5), then the system is consistent but overspecified and a hydrostatic pressure mode will exist. The latter, if the only pressure mode present, can be eliminated with no adverse effects by specifying the pressure at one "node" in the system. A contained flow is a common example wherein the pressure is only determined up to an arbitrary additive constant.

3. Finally, if the imposed BC's violate equation (5), which can only occur (as in 2 above) if the normal velocity is specified everywhere on the boundary, then the discretized system is inconsistent and no solution is possible.

B. The Checkerboard Mode

Here one asks the question: Are there, in addition to the above hydrostatic case, any other linear combinations of the M continuity equations which can result in a boundary node constraint equation? In order to answer this question, we use some of the ideas presented in [12] and [13]. For the simple grid of parallelograms displayed in Fig. 2, a slight generalization of Fig. 1, consider, for the moment, the continuity equation associated with element #1. It can be cast in the form

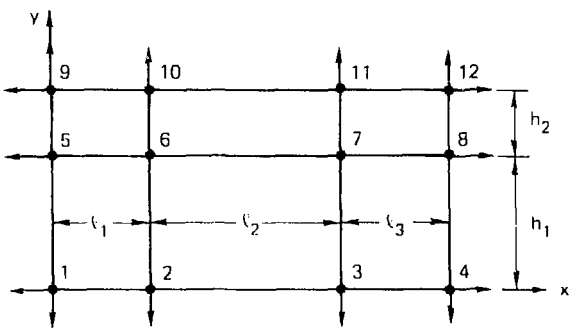

Figure 1

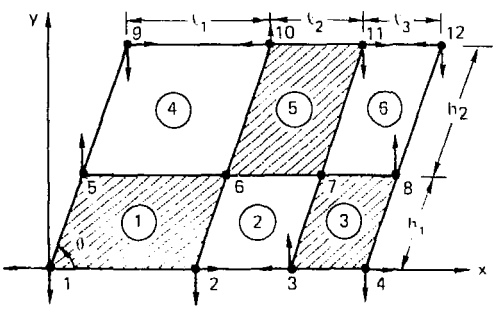

Figure 2

$$\frac{(u_2-u_1+u_6-u_5)}{\ell_1} + \frac{(v_5-v_1+v_6-v_2)}{h_1 \sin\theta} + \frac{(v_5-v_2+v_1-v_6)}{\ell_1 \tan\theta} = 0 \qquad (7)$$

by dividing its original form by the area of element #1 ($\ell_1 h_1 \sin\theta$). Recasting all of the continuity equations associated with the grid of Fig. 2 into this form by dividing by the appropriate element areas, the following "CB equation" can be obtained from the original set of continuity equations:

$$\sum_{i=1}^{M_B} C_{B_i}/A_i - \sum_{i=1}^{M_R} C_{R_i}/A_i = 0 \quad , \qquad (8)$$

where C_{B_i}, C_{R_i} are interpreted to mean the discretized continuity equation for the i-th black, or red, element, M_B, M_R are the total number of black, or red, elements ($M_B+M_R = M$), and A_i is the area of the i-th element. A closer inspection of Eqn. (8) reveals that it does, in fact, represent a constraint among only boundary nodes on the grid of Fig. 2; or, in fact, on any grid composed of arbitrary-sized parallelograms with constant angle θ. For the important special case of rectangles ($\theta = \pi/2$), the constraint equation relates tangential velocities on the boundary. (See [10], for a more detailed discussion). It is noteworthy that the constraint Eqn. (8) does not

eliminate all interior nodes on a general mesh with distorted isoparametric elements (or any mesh containing "bent lines"). In the special, but important case of constant θ, the boundary constraint equation is, as in the hydrostatic case, the reason for the existence of a (spurious) CB pressure mode. Noting that Eqn. (8) must be satisfied regardless of the applied BC's (again temporarily ignoring the possibility of other pressure modes) leads to:

1. If the imposed BC's do not imply a constraint among the velocities on the entire boundary, then the constraint Eqn. (8) is independent and required and no spurious CB mode occurs. However, the resulting "boundary equation" (8) generated by the continuity equations is extraneous (in contrast to that corresponding to the hydrostatic mode).

2. If the imposed BC's duplicate the constraint Eqn. (8), the system is consistent, but over-specified. A spurious CB pressure mode exists and, contrary to the hydrostatic mode, it cannot be eliminated by specifying a "nodal" pressure (which is nevertheless legitimate and removes the rank deficiency) and it can lead to non-physical constraints.

3. Finally, if the imposed BC's violate Eqn. (8), the discretized system is ill-posed and no solution is possible.

In concluding this discussion it should be pointed out that there is a possibility of the simultaneous existence of both pressure modes since constraint Eqns. (5) and (8) are always present (there are but two pressure modes for this element) and concomittantly, the possibility of ill-posedness due to a violation of either constraint equation. In this case, as in the previous case, post-processing will be required to filter the spurious CB mode. Also note here that specification of the pressure at two points in the flow field (one on any black element, the other on any red) will remove the rank deficiency and, while physically absurd, is mathematically permissible - a manifestation of the spurious CB mode.

C. Description of the Pressure Modes

The existence of a pressure mode can be recast in terms of the existence of a zero eigenvalue for the eigenvalue problem associated with (4), i.e.,

$$\underline{\underline{K}}\,\underline{w}_i + \underline{\underline{C}}\,\underline{r}_i = \lambda_i\,\underline{w}_i \quad , \quad \underline{\underline{C}}^T\underline{w}_i = \lambda_i\,\underline{r}_i \quad , \tag{9a, 9b}$$

where λ_i are the eigenvalues and $(\underline{w}_i^T \quad \underline{r}_i^T)^T$ the corresponding eigenvectors, i = 1, 2, ..., N + M. A pressure mode corresponds to a solution to (9) of the form

$$\lambda_i = 0 \quad , \quad \underline{w}_i = 0 \quad , \quad \underline{\underline{C}}\,\underline{r}_i = 0 \quad , \tag{10}$$

where $\underline{r}_i$ is the pressure mode - and our goal here is to describe its form.

(1) Hydrostatic Pressure Mode

Here the eigenvector corresponding to the hydrostatic mode is simply $\underline{r} = \underline{P}_H$, where $\underline{P}_H$ is an arbitrary constant vector. The proof follows directly from the definition of

$$\underline{\underline{C}}\,\underline{P}_H \equiv ((\underline{\underline{C}}_x\underline{P}_H)^T \quad (\underline{\underline{C}}_y\underline{P}_H)^T)^T \qquad \text{where}$$

$$-(\underline{\underline{C}}_x\,\underline{P}_H)_i = \sum_{j=1}^{M} P_j \int_\Omega \frac{\partial \phi_i}{\partial x}\,\psi_j\,dxdy = P_H \int_\Omega \frac{\partial \phi_i}{\partial x}\,dxdy = P_H \int_{\partial\Omega} \phi_i\,dy \tag{11}$$

and $(\underline{\underline{C}}_y\,\underline{P}_H)_i$ can be generated by an interchange of x and y in (11) and changing the sign of the final result. Consequently, the conditions under which $\underline{\underline{C}}\,\underline{P}_H = \underline{0}$ are:

1. If u and v are specified everywhere on $\partial\Omega$, $\phi_i = 0$ on $\partial\Omega$ and each component of (11) vanishes. A contained flow always displays a hydrostatic mode.

2. If all of $\partial\Omega$ has the normal velocity component and the tangential force prescribed. (See [10] for details).

In general, a hydrostatic mode exists under any combination of the above two boundary condition types (and only these types).

(2) Checkerboard Pressure Mode

If the i-th equation of (2b) is multiplied by the coefficient

$$\underline{r}_i = p_i^C = \pm\, 1/A_i \quad \text{(the CB eigenvector)} \quad , \tag{12}$$

where A_i is the area of the i-th element, the plus sign corresponding to a "black" element and the minus sign to a "red," an equation similar in form to (11) is obtained. The resulting equation can be used to generate the following results, which are detailed in [10] (the CB eigenvector also satisfies Eqn. 10):

1. For a general, arbitrarily-oriented grid of parallelograms, a CB mode can exist only if all boundary velocities are specified (e.g., contained flow).

2. For a grid of parallelograms oriented so that two sides are parallel to the x-axis, a CB mode can also exist if u is 'free' along the two sloped sides. There also exists the counterpart for a grid aligned with the y-axis; however, neither of these cases is of much practical interest since the associated boundary conditions are not the physically relevant ones.

3. For a grid of arbitrary-sized rectangles a CB mode can also exist when the tangential components of velocity are prescribed over the entire boundary, a situation which may be more commonly encountered in practice. An example of such a CB situation is displayed in Fig. 3. If the tangential boundary condition at the right side is changed from $v = 0$ to $f_t = 0$ (i.e., specified shear stress), the CB mode could no longer exist.

Finally, it is noteworthy that the existence of a CB mode can preclude the existence of a solution to the algebraic system; there are, in fact, common situations (see Ex. 2 below) in which a CB mode exists, but the solution to the discretized Navier-Stokes equations does not exist. The "converse" is also true in that the nonexistence of the CB mode is a sufficient condition for the existence (and uniqueness) of a solution to the algebraic system (in the absence of the hydrostatic mode).

D. Further Implications of the Spurious Constraint

The fact that the "CB constraint equation," (8), must always be satisfied by the discretized solution carries other, rather serious implications, over and above the possible existence of a CB mode. We will demonstrate two consequences of this extraneous constraint via simple examples. In the first example, the (extraneous) constraint on boundary velocities occurs in a flow which has no CB mode and, in the second example, it occurs in conjunction with the CB mode and can lead to an ill-posed problem.

Example 1: Tangential Velocity Constraints

We begin by returning to the grid in Fig. 3 and modifying the 'outflow' boundary condition from $v = 0$ to $f_t = 0$, so that no CB mode can exist. However, application of the CB constraint equation to this grid gives, considering the imposed boundary conditions,

$$(\frac{1}{h_1} + \frac{1}{h_2})v_1 - (\frac{1}{h_2} + \frac{1}{h_3})v_2 + (\frac{1}{h_3} + \frac{1}{h_4})v_3 + \ldots \pm (\frac{1}{h_N} + \frac{1}{h_{N+1}})v_N = 0 \quad . \tag{13}$$

The existence of this spurious constraint equation, which will be satisfied by the numerical solution, is an artifact of the discretization with the bilinear element and it exists independently of, and in addition to, the proper constraints; viz, those imposed by the shear-free boundary condition and global mass conservation. If this 'element' converges to the solution of the (Navier-)Stokes equations, this constraint is presumably not too 'harmful' (our numerical simulations which do, in fact, satisfy (13), appear 'reasonable') and in fact, must vanish as $h \to 0$. Finally, if v is specified at the outflow such that (13) is violated, the problem is ill-posed and no solution exists.

Example 2: The Driven Cavity

The popular lid-driven cavity problem is an appropriate example to demonstrate another important consequence of the "CB constraint," and is depicted in Fig. 4.

Application of (8) to this grid gives a different result, depending on whether N-1 (the number of elements across the top of the cavity) is even or odd: For N-1 even,

$$\frac{1}{\ell_1}u_1 - (\frac{1}{\ell_1} + \frac{1}{\ell_2})u_2 + (\frac{1}{\ell_2} + \frac{1}{\ell_3})u_3 - \ldots - (\frac{1}{\ell_{N-2}} + \frac{1}{\ell_{N-1}})u_{N-1} + \frac{1}{\ell_{N-1}}u_N = 0 \quad (14a)$$

and for N-1 odd,

$$\frac{1}{\ell_1}u_1 - (\frac{1}{\ell_1} + \frac{1}{\ell_2})u_2 + (\frac{1}{\ell_2} + \frac{1}{\ell_3})u_3 - \ldots + (\frac{1}{\ell_{N-2}} + \frac{1}{\ell_{N-1}})u_{N-1} - \frac{1}{\ell_{N-1}}u_N = 0 \quad . \quad (14b)$$

Consider first the simpler case in which $u_i = u_o$, i = 1, 2 ... N; i.e., the case of equal velocity at every node, including the first and last (a 'flow-through' cavity). In this case, both (14a) and (14b) are satisfied identically (i.e., the CB constraint is automatically satisfied for either an even or odd mesh and a CB mode will exist). If, however we wish to compute the more difficult case of a contained flow, we might set $u_1 = u_N = 0$ and $u_i = u_o$, i = 2, 3, ..., N-1. In this case we obtain

$$-u_o(\frac{1}{\ell_1} + \frac{1}{\ell_{N-1}}) = 0 \qquad \text{for an even grid,}$$

and

$$u_o(-\frac{1}{\ell_1} + \frac{1}{\ell_{N-1}}) = 0 \qquad \text{for an odd grid.}$$

While the constraint equation on an odd grid can be satisfied if $\ell_1 = \ell_{N-1}$ (in which case the CB pressure mode, as well as the hydrostatic mode, exists), it can never be satisfied on an even grid. Hence, the driven cavity problem, for these (mathematically permissible) boundary conditions, is ill-posed on any grid with an even number of elements across the top and on any odd-element grid which doesn't satisfy $\ell_1 = \ell_{N-1}$. These are clearly physically erroneous constraints and are forced upon the discretized system by the extraneous CB pressure mode. An even grid can, if desired, be employed for a contained flow simulation ($u_1 = u_N = 0$), if the proper precautions are taken: e.g., for $u_i = u_o$; i = 3, 4, ... N-2, (14) can be easily satisfied (e.g., for ℓ = constant, $u_2 + u_{N-1} = u_o$ will suffice, and it is then reasonable to take $u_2 = u_{N-1} = 1/2\ u_o$; we have used this approach successfully and have presented results in [6]).

The net result, as demonstrated by these two examples, is that the CB constraint is rather insidious, far-reaching, and probably even has important implications regarding the ultimate proof of convergence of this FEM approximation (which proof, according to [14], is "still an open question" - perhaps it must remain that way).

E. The Impure Checkerboard Pressure Mode

We now address the most difficult of the pressure mode effects which we have encountered: one might optimistically expect, since the existence of the CB mode was proven under somewhat specialized conditions (a mesh of parallelograms), that it would not occur under the more general conditions of a mesh composed of variously distorted isoparametric elements. Unfortunately, this is not the case; in fact, a 'residual' CB pattern appears to be present (under appropriate boundary conditions; viz., those which permit the existence of a "pure" CB mode) even in a mesh composed of arbitrarily distorted isoparametric elements. However, since it does not display characteristics identical to the pure CB mode, we have labeled this an "impure" CB mode.

Basically, the impure CB mode appears to exist in such a way that, while not pure (there is no corresponding zero eigenvalue in the matrix with an associated pure pressure eigenvector - other than the hydrostatic pressure mode - and therefore, no associated

redundant continuity equation), the pressure solution is still oscillatory and generally unacceptable without further post-processing. Our explanation of the impure mode (which appears to explain essentially all of the results from a wide variety of numerical experiments) is one which considers it as a perturbation from the simpler pure CB mode and it is this approach which we shall present; i.e., any mesh which is not composed of parallelograms is to be interpreted as a perturbation (small in theory, but not necessarily in practice) from one which is. The original CB theory is only partially applicable in that it would predict that the perturbed matrix would no longer have a zero eigenvalue (correct) and that a CB pressure mode would no longer exist (incorrect). It is toward the reconciliation of this, and similar issues, that we present the results of an approximate (linearized) perturbation analysis of the impure CB mode.

The analysis (see [10] for details) is performed on a perturbed version of (4) in which $\underline{\underline{K}} \to \underline{\underline{K}} + \delta\underline{\underline{K}}$, $\underline{\underline{C}} \to \underline{\underline{C}} + \delta\underline{\underline{C}}$, $\underline{f} \to \underline{f} + \delta\underline{f}$ and $\underline{g} \to \underline{g} + \delta\underline{g}$ and a parameter ε, which is a measure of the perturbation (i.e., $|\delta\underline{\underline{K}}| \sim O(\varepsilon)$, etc.). For example, ε could be associated with the departure of the elements of the grid from parallelograms, as in one of the examples presented in [10]. The results are:

1. The CB eigenvector $(\underline{0} \quad \underline{r}_C^T)^T$ is projected from the original null space into the space of the remaining perturbed eigenvectors, in specific but small $O(\varepsilon)$, amounts.

2. The impure CB eigenvector contains, in addition to the pure pressure mode, small amounts ($O(\varepsilon)$) of the velocity and pressure portions of all other eigenvectors.

3. All eigenvalues are perturbed to $O(\varepsilon)$ except the CB eigenvalue, which is perturbed to $O(\varepsilon^2)$. Moreover, all eigenvectors are perturbed to $O(\varepsilon)$, which leads to the presence of the original CB mode to a "large" extent ($O(1/\varepsilon)$) in the "perturbed" pressure solution; concomitantly, the velocity field is perturbed to O(1) (an unfortunate, but true result).

4. Since the $\varepsilon \to 0$ limit is a singular one, the $(1/\varepsilon)$ behavior must be interpreted to mean that the impure CB mode approaches the pure CB mode with an arbitrary amplitude coefficient as $\varepsilon \to 0$.

In spite of the difficulties associated with the singular limit, these results have been corroborated by our numerical results as illustrated in [10].

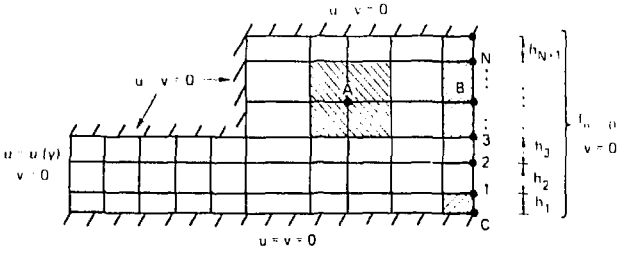

Figure 3

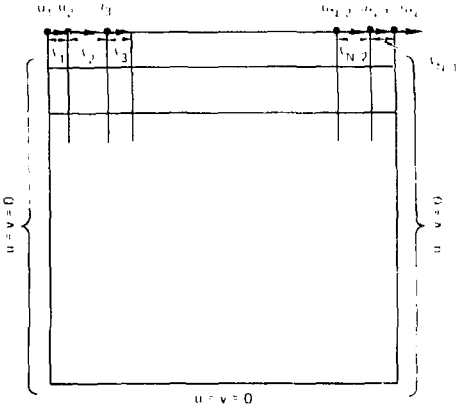

Figure 4

F. Filtering and Smoothing Techniques

Since the CB pressure mode has been shown to be quite persistent, it must be filtered from the physical part of the pressure solution if usable pressure results are to be obtained. The two schemes which we have developed to filter this pressure mode are directly related to a knowledge of the form of the CB eigenvector, and (in the first scheme) the fact that this eigenvector is, in some sense, orthogonal to the integral of a bilinear basis function. (See [10] for details).

The CB filtering (and 'smoothing') techniques described here each generate a smoothed (physical) pressure at a node (i) joined by an even number of elements. The reason we refer to the pressures as 'smoothed' is that they are now available at the velocity nodes rather than at the element centroids, and can, if desired, be considered as continuous functions via representation by the velocity basis functions, $\{\phi_i\}$.

(1) Basis Function Weighting

In this scheme

$$P_i = \int_\Omega p^h \phi_i \, dxdy / \int_\Omega \phi_i \, dxdy \quad , \tag{15}$$

where p^h is the pressure obtained from Eqns. (3) and (4).

The associated nodal pressure field gives a best fit (based on $\{\phi_i\}$) in a modified least squares sense over the domain Ω. Details and examples are presented in Lee et al. [6].

(2) Area Weighting

Here

$$P_i = \frac{1}{A} \sum_e P_e A_e \quad , \tag{16}$$

where A is the total area of the elements sharing node (i), P_e is the polluted computed pressure, A_e is the area associated with element 'e', and the sum is over all elements sharing node i. (For either filtering scheme, "corner nodes" must receive special attention as described, for example in [5] or [6]). In our experience both filters have been successful in filtering not only the pure CB mode on a regular mesh of parallelograms, but also the impure CB mode on irregular meshes. The latter method is obviously simpler and concomitantly, more cost effective, than the basis-function averaged scheme and hence is to be recommended (the two methods give identical results for pure CB modes).

Two additional noteworthy features of the latter scheme are:

1. It is directly extendible to the three-dimensional (FEM) case.
2. Caldwell [7] has used this technique to successfully smooth a CB mode obtained when using the 3D BAAL finite difference code [9]).

GENERALIZATION TO OTHER ELEMENTS

While theory (see, for example, [15] and [16]) provides, under certain hypotheses, an existence and uniqueness proof for the continuum Navier-Stokes equations in certain function spaces, the GFEM approximation in the same spaces can, as illustrated in previous sections, suffer from non-uniqueness and even non-existence. This situation arises due to the existence of spurious pressure modes in the pressure approximation space. In order to gain additional insight into such problems, it is necessary to extend the previous investigation of "pure" pressure modes to more complicated mixed- and equal-order interpolation elements, and this leads naturally to an investigation of the uniqueness and existence of the GFEM approximation of the problem in its natural function space setting.

A. Theory

The formulation of the Stokes problem can be cast in the following form:

$$(p^h, \nabla \cdot \underline{w}^h) = A(\underline{u}^h, \underline{w}^h) \quad , \qquad (\nabla \cdot \underline{u}^h, q^h) = 0 \tag{17, 18}$$

for all $\underline{w}^h \in W_{h,o}$, $q^h \in Q_h$. Here

$$(a,b) \equiv \int_\Omega ab \quad , \qquad A(\underline{u},\underline{w}) \equiv \int_\Omega (\nabla \underline{w})^T : S(\underline{u}) \quad , \tag{19, 20}$$

$W_{h,o}$ is a finite dimensional space of C^o vector functions on Ω with vanishing components on those parts of the boundary on which the associated velocity components are specified, and Q_h is a finite dimensional subspace of functions which form a basis for the space of all square integrable functions on Ω ; i.e., $L_2(\Omega)$. The usual GFEM subspaces Q_h are either *piecewise continuous* (C^o) *or piecewise discontinuous* (C^{-1}) polynomials. The previous considerations on the linear velocity - constant pressure element can be recovered and generalized by investigating the uniqueness and existence of the GFEM solution.

Addressing the uniqueness question leads to the following result, whose development is detailed in [10];

Condition A:

For all $\underline{w}^h \in W_{h,o}$,

$$(\nabla \cdot \underline{w}^h, p^h) = 0 \tag{21}$$

must imply $p^h = 0$ if the Galerkin finite element pressure field is to be unique. If solutions to (21) exist with $p^h \neq 0$, (i.e., if Condition A is violated) the GFEM solution is non-unique and pressure modes will exist even though a unique velocity field is obtained.

It is noteworthy that the latter condition is also a restriction appropriate to the GFEM Navier-Stokes problem because it is generated by setting $\underline{u}^h = \underline{0}$ and the nonlinear terms vanish. The hydrostatic pressure mode obviously violates Condition A and, being acceptable physically, can be incorporated by recasting Condition A to read p^h = constant. Condition A appears to be a special case of a result due to Brezzi [17] for saddle point variational problems and furthermore, one of its consequences is that the computation of the eigenvalues of an element matrix as, for example, carried out by Olson and Tuann [2] is insufficient for the investigation of pressure modes.

When pressure modes exist, certain solvability conditions must also be satisfied by the GFEM system. These are generated by setting $(\underline{w},q) = (0, p^h_{ci})$, i.e., the pressure modes, in the Galerkin formulation, (17)-(18), which leads to

Condition B:

$$(\nabla \cdot \underline{u}^h, p^h_{ci}) = 0 \quad ; \qquad i = 1, 2, \ldots n \quad , \tag{22}$$

where n is the total number of pressure modes. If this condition is violated, the associated GFEM system is inconsistent and has no solution.

B. Applications

(1) The Linear Velocity-Constant Pressure Element. The utilization of the foregoing conditions can be illustrated by applying it to the previously considered case of the linear velocity - constant pressure element. The satisfaction of Condition A is implemented in this case by setting

$$\underline{w}^h = \begin{pmatrix} C_1 \\ C_2 \end{pmatrix} \phi^h \quad , \tag{23}$$

where ϕ^h is an arbitrary piecewise bilinear velocity basis function and C_1 and C_2 are arbitrary constants, and by requiring any possible pressure modes to be independent of the choice of basis function. The three relevant forms are illustrated in Fig. 3 by nodes A, B and C and their corresponding shaded supports. It is apparent that associated with interior nodes (node A) are velocity basis functions with support over a four-patch of neighboring elements and that basis functions with one- or two-patch supports are associated with boundary nodes (nodes B and C, respectively). (The one and two patch cases do not have to be considered if the problem has purely Dirichlet boundary data since these degrees of freedom do not appear in $W_{h,o}$). The invariance of the possible pressure modes to the velocity basis functions $\underline{w}^h$ appearing in (23) can be satisfied by

requiring the four-patch (one- or two-patch) results to be "patch -independent." That is, the results must be simultaneously applicable to every such patch (basis function) associated with the mesh. This restriction can be used to establish that the CB mode can only exist on meshes generated by straight parallel lines. Consequently, only the general four-patch displayed in Fig. 5a need be considered. (In Fig. 5, θ is the same angle defined in Fig. 2).

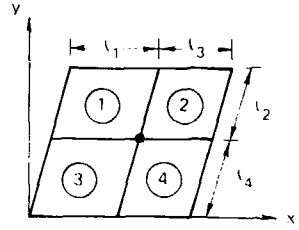

(a) Four-patch

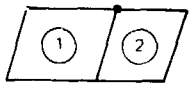

(b) Two-patch

(c) One-patch

Figure 5

Substituting (23) into (21), coupled with a piecewise constant pressure field, yields

$$\ell_2(p_1-p_2) + \ell_4(p_3-p_4) = 0 \quad , \tag{24}$$

$$-(\ell_1+\ell_2\cos\theta)p_1 - (\ell_3-\ell_2\cos\theta)p_2 + (\ell_1-\ell_4\cos\theta)p_3 + (\ell_3+\ell_4\cos\theta)p_4 = 0 \quad . \tag{25}$$

The only solutions to (24) and (25) which are patch-independent are the hydrostatic mode and the CB mode. Here it is apparent that invariance is guaranteed since the amplitude of the CB mode on an element depends only on the area of that element. If the problem being considered is one in which the velocity is specified everywhere on the boundary, i.e., Dirichlet type boundary data, the existence of a checkerboard mode has been established. On the other hand if normal force, or traction-type conditions are specified on the boundary, then it is necessary to check that any possible patch-invariant pressure modes associated with the four-patch are also compatible with any one- or two-patch associated with a boundary degree of freedom in the velocity field. The three different combinations of boundary conditions of interest and the corresponding restrictions imposed by applying (21) on the two-patch of Fig. 5b (whose dimensions correspond to those in Fig. 5a for elements 1 and 2) are:

$$f_n,u_t \text{ specified: } \ell_1 p_1 + \ell_3 p_2 = 0 \quad ; \qquad f_t,u_n \text{ specified: } (p_1-p_2) = 0 \tag{26, 27}$$

$$f_t,f_n \text{ specified: } (p_1-p_2) = 0 \quad , \qquad \ell_1 p_1 + \ell_3 p_2 = 0 \quad . \tag{28, 29}$$

A perusal of these constraints establishes that the hydrostatic mode does not satisfy (26) and (29) and the CB mode does not satisfy (27) and (28). Consequently, it follows that specification of f_t on <u>any</u> part of the boundary will annihilate the pure CB mode; it also follows that if f_n is additionally specified on any part of the boundary, the hydrostatic mode is annihilated and there is no longer any indeterminancy in the "physical" pressure field. In this case, the pressure may not be specified anywhere in, or on, the domain - a result which can be shown to be independent of the velocity basis and valid in general. In addition, the requirement of compatibility of possible pressure modes with any degrees of freedom associated with a one-patch, as illustrated in Fig. 5c, establishes that if such velocity degrees of freedom exist, the pure CB mode does not exist. Thus, only if the velocity is specified at a corner node of a domain can the pure CB mode occur if it is otherwise allowable. Finally, the solvability constraints previously generated for the linear velocity-constant pressure element can be duplicated here by applying Condition B to the CB mode (an exercise we leave to the reader).

(2) Equal-Order Interpolation Elements. In order to illustrate the application to equal order interpolation elements, the C^0 bilinear velocity-bilinear pressure (C^0 or C^{-1}) interpolation will now be considered. In the discontinuous pressure case, the pressure interpolation employs (2x2) Gauss point pressures. In order to demonstrate the existence of pressure modes, it is only necessary to demonstrate a violation of Condition A. Here again pure pressure modes are found to be restricted to meshes generated by parallel straight lines. An isoparametric finite element is used and each of the quadrilateral elements in Fig. 5 is mapped onto the reference square $[-1, -1] \leq (\xi,\eta) \leq [1, 1]$. A violation of Condition A can be demonstrated by setting

$$p_i^h = D_i \eta \quad , \qquad \underline{w}^h = \begin{pmatrix} C_1 \\ C_2 \end{pmatrix} \underline{\phi}^h(\xi,\eta) \quad ,$$

where p_i^h of Q_h is a portion of the bilinear pressure in element i, D_i is an arbitrary constant in element i, and $\underline{\phi}^h(\xi,\eta)$ is the appropriate velocity basis function.

For this case, application of (21) to the four-patch of Fig. 5a leads to

$$\int p^h \nabla \cdot \underline{w}^h = \sum_{i=1}^{4} \int_{\Omega_i} p_i^h \nabla \cdot \underline{w}^h = \sum_{i=1}^{4} D_i \int_{-1}^{1}\int_{-1}^{1} \eta [C_1(\alpha_i+\beta_i\eta) + C_2(\gamma_i+\delta_i\xi)] \, d\xi d\eta = 0 \quad (30)$$

where α_i, β_i, γ_i and δ_i are constants associated with the mapping of element i into the reference square. Note that the integrals in (30) are identically zero for arbitrary constants (C_1, C_2, D_i) because all integrands are odd functions in either ξ or η. By restricting the index "i" in (30) to 2 or 1, one generates the form of the integral for a typical boundary two- or one-patch, respectively. Therefore, the same conclusion holds in these cases. Consequently, Condition A is violated not only in the C^0 bilinear pressure approximation case, but also in the discontinuous (C^{-1}) bilinear case. (The pressure mode $p_i^h = D_i\xi\eta$ corresponds to a C^0 approximation if the magnitude of D_i is the same for all elements in the patch but its sign is different for any two adjacent elements sharing a node; otherwise, p_i^h is a piecewise discontinuous (C^{-1}) approximation. The same reasoning can be applied to the functions $p_i^h = D_i\xi$ or $p_i^h = D_i\eta$ which appear below). Moreover, here the violation of Condition A, and hence the occurrence of at least one spurious pressure mode, is independent of the prescribed velocity boundary conditions because the boundary one- and two-patch (velocity basis functions which would be associated with boundary nodes) result is independent of C_1 and C_2.

Replacement of p^h appearing in the integral in (30) successively by D_i = const., $D_i\xi$, and $D_i\eta$ can be used to further establish that at least the physical hydrostatic pressure mode, a spurious plane "ξ-wave" pressure mode and a spurious plane "η-wave" pressure mode, respectively, are also possible in the C^0 pressure approximation case. For the ξ- and η-modes, Condition A is not violated automatically because of an odd integral as in the $\xi\eta$-mode case, but by satisfaction of certain constraints by these waves. In these cases, violation of Condition A on a "four-patch" requires that

$$(1) \quad p_i^h = D_i\xi \;:\; D_1 = D_4, D_3 = D_2; \qquad (2) \quad p_i^h = D_i\eta \;:\; D_1 = D_2, D_3 = D_4. \quad (31)$$

Condition (1) is satisfied by a ξ-wave on any four-patch in the grid and Condition (2) is similarly satisfied by the η-wave. The inclusion of a one- and two-patch test, which reflects the specification of normal or tangential forces on the boundary, establishes that the ξ-wave and η-wave pressure modes can be suppressed if the force normal to the wave form is specified on a portion of the boundary. Consequently, in general multiple degeneracies must occur when using this element to simulate flows in which the velocity is specified everywhere on the boundary. In fact, on a sufficiently large mesh of elements (where momentum equations sufficiently exceed continuity constraints), we have found seven spurious pressure modes numerically; the C^{-1} bilinear pressure case will be even more degenerate because of an excess of continuity constraints compared to momentum constraints.

(3) The Biquadratic Velocity-Bilinear Pressure Element. Finally, a very accurate and useful element which is afflicted with one spurious pressure mode is that defined by biquadratic (9-node) velocity and discontinuous bilinear pressure (at the 2x2 Gauss points). For a description of the pressure mode and a useful filter for this element, see [10].

REMARKS ON EARLIER THEORY AND THE PENALTY APPROACH

Focusing on the GFEM formulation, certain earlier analyses provide, for example, hypotheses under which the scheme converges to a unique solution as well as error estimates. In [15] and [16] a finite element mesh composed of non-degenerate triangles is considered and both general results and results for specific elements is provided; [18] and [19] provide less detailed results applicable to a class of elements. Most of these results, including existence and uniqueness, appear to be applicable to the Lagrange family of quadrilateral elements. Consequently, one must rationalize the existence of pressure modes, i.e., non-uniqueness in the approximate pressure field, and, for example, the theoretical results establishing uniqueness. Moreover, as demonstrated herein, the solvability constraints imposed on the discrete problem by the spurious pressure modes can force the allowable boundary conditions to be mesh dependent - a constraint which raises the fundamental question of convergence of the method. Finally, the equivalence of the mixed interpolation GFEM employing a discontinuous pressure approximation space (with Gauss point nodes) and the penalty approach via GFEM (see [20]) must be questioned in general. More details on these issues can be found in [10].

NUMERICAL EXAMPLES

During this investigation a sufficient number of numerical experiments (well over one hundred) were conducted to corroborate the theory. A selected set will be presented at the meeting and a summary will appear in [10].

SUMMARY AND CONCLUSIONS

We have explained the cause of the spurious pressures generated when the GFEM is applied to the incompressible Navier-Stokes equations. Some of the implications of the spurious pressure modes were also described. Finally, we have shown that useful pressure fields can nevertheless be obtained, in some cases, via appropriate filtering and smoothing schemes, applied in a "post-processing" manner.

ACKNOWLEDGMENTS

R.L.S. would like to acknowledge support from both Lawrence Livermore Laboratory and the U.S. Army Research Office (Grant DAAG29-79-6-0045). This work was performed under the auspices of the U. S. Department of Energy by the Lawrence Livermore Laboratory under contract No. W-7405-Eng-48.

REFERENCES

1. Hood, P. and C. Taylor, "A Numerical Solution of the Navier-Stokes Equations Using FEM Technique," Comp. and Fluids, 1, 73-100, 1973.

2. Olson, M. and S. Tuann, "Primitive Variables Versus Stream Function Finite Element Solutions of the Navier-Stokes Equations," Finite Elements in Fluids, 3, 73-89, John Wiley & Sons, Ltd., New York, 1978.

3. Fabayo, O. R., "Bilinear Finite Elements for Incompressible Flow," M.Sc. Dissertation, Dept. Math., University of Dundee, Scotland, 1977.

4. Huyakorn, P. A., C. Taylor, R. L. Lee and P. M. Gresho, "A Comparison of Various Mixed Interpolation Finite Elements in the Velocity-Pressure Formulation of the Navier-Stokes Equations," Computers and Fluids, 6, 25-35, 1978.

5. Hughes, T.J.R., W.K. Liu and A. Brooks, "Finite Element Analysis of Incompressible Viscous Flows by the Penalty Formulation," J. Comp. Phys., 39, 1-15, 1979.

6. Lee, R. L., P. M. Gresho and R. L. Sani, "Smoothing Techniques for Certain Primitive Variable Solutions of the Navier-Stokes Equations," to appear Int. J. Num. Methods in Engng., 1979.

7. Caldwell, C., Westinghouse Electrical Corporation, Pittsburgh, PA, Private communication, 1979.

8. Fortin, M., "Numerical Solution of Steady State Navier-Stokes Equations," Numerical Methods in Fluid Dynamics, J. J. Smolderen (editor), Agard Lecture Series No. 48, AGARD-LS-48, 1972.

9. Pracht, W. E. and J. V. Brackbill, "BAAL: A Code for Calculating Three-Dimensional Fluid Flows at all Speeds with an Eulerian-Lagrangian Computing Mesh," Los Alamos Scientific Laboratory Report LA-6342, 1976.

10. Sani, R. L., P. M. Gresho, R. L. Lee and D. F. Griffiths, "The Cause and Cure of the Spurious Pressures Generated by Certain GFEM Solutions of the Incompressible Navier-Stokes Equations," to appear Int. J. Num. Methods in Fluids, 1980.

11. Gresho, P. M., R. L. Lee and R. L. Sani, "On the Time-Dependent Solution of the Incompressible Navier-Stokes Equations in Two and Three Dimensions," to appear Recent Advances in Numerical Methods in Fluids, Pineridge Press.

12. Meehan, T. P., "Some Aspects of the Finite Element Method for Slow, Viscous Flow Problems," M.Sc. Dissertation, Dept. Math., University of Dundee, Scotland, 1976.

13. Richards, G. D., "Finite Elements for Incompressible Flow," M.Sc. Dissertation, Dept. Math., University of Reading, UK, 1978.

14. Fortin, M., "An Analysis of the Convergence of Mixed Finite Element Methods," RAIRO, 11, R-3, 341-354, 1977.

15. Crouizeix, M. and P. A. Raviart, "Conforming and Nonconforming Finite Element Methods for Solving the Stationary Stokes Equations I," RAIRO, R-3, 33-76, 1973.

16. Jamet, P. and P. A. Raviart, "Numerical Solution of the Stationary Navier-Stokes Equations by Finite Element Methods," Lecture Notes in Computing Sci. Part 1, 193-223, G. Goos and J. Herimanis (editors), Springer-Verlag, 1974.

17. Brezzi, F., "On the Existence, Uniqueness and Approximation of Saddle Point Problems Arising from Lagrangian Multipliers," RAIRO, 8, R-2, 129-151, 1974.

18. Bercovier, M., "Perturbation of Mixed Variational Problems. Application to Mixed Finite Element Methods," RAIRO, 12, 211-236, 1978.

19. Reddy, J. N., "On the Accuracy and Existence of Solutions to Primitive Variable Models of Viscous Incompressible Fluids," Int. J. Engng. Sci., 16, 921-929, 1978.

20. Bercovier, M. and M. Engelman, "A Finite Element for the Numerical Solution of Viscous Incompressible Flow," J. Comp. Phys., 30, 181-201, 1979.